Does the Collagen Network Contribute to Normal Systolic Left Ventricular Wall Thickening? A Theoretical Study in Continuum Mechanics

Jacques Ohayon[1], Christian Bourdarias[2], and Stéphane Gerbi[2]

[1] Laboratoire TIMC-IMAG, Equipe DynaCell, Domaine de la Merci
38706 Grenoble cedex, France
Jacques.Ohayon@imag.fr
http://timc.imag.fr/dynacell
[2] Université de Savoie, LAMA, 73376 Le Bourget-du-Lac, France

Abstract. Studies in mammalian hearts shown that left ventricular wall thickening is an important mechanism for normal systolic ejection, and that during contraction the myocardium develops a significant stress in the muscular cross-fiber direction. We suggested that the collagen network surrounding the muscular fibers could account for these two mechanical behaviors. To test this hypothesis, we developed a mathematical model for a large deformation response of an active, incompressible, hyperelastic and transversely isotropic cardiac tissue, in which we included a coupling effect between the connective tissue and the muscular fibers. The three-dimensional constitutive law containing this internal pseudo-active kinematic constraint is derived and applied to obtain solutions for the cases of a free contraction, uniaxial and equibiaxial extensions of a rectangular sample assuming negligible body forces and inertia effects. This model may explain the contribution of the collagen network to the two following mechanics: (i) the normal systolic wall thickening, and (ii) the developed pseudo-active tension in the cross-fiber direction.

1 Introduction

It is known, that the transverse shear along myocardial cleavage planes provides a mechanism for a normal systolic wall thickening [5]. Indirect evidences indicate that the characteristics of the passive extracellular connective tissue in the myocardium is an important determinant of ventricular function ([6], [10], [3]). An appropriate constitutive law for the myocardium should therefore incorporate the most important features of its microstructure. A sound theoretical formulation for material laws of the active myocardium is essential for an accurate mechanical analysis of the stresses in the ventricular wall during the whole cardiac cycle. The wall stress distribution is one of the main factors governing the myocardial energetic [11], the coronary blood flow [2], the cardiac hypertrophy [10], and the fetal heart growth [7]. To date we do not have any reliable technique

I. Magnin et al. (Eds.): FIMH 2003, LNCS 2674, pp. 91–100, 2003.

to evaluate the stress in the cardiac muscle, therefore, mechanical models are useful in cardiology to assess the functional capacities of the human heart. Several numerical models using a finite element (FE) analysis have been performed to simulate the left ventricular performance ([4], [13]). The mechanical behavior of the connective tissue is often assumed isotropic [8]. This last assumption is not in agreement with the experimental results obtained on a sample of active myocardial rabbit tissue. Lin and Yin [6] showed that, during an active equibiaxial stretch test, there are significant stresses developed in the cross-fiber direction (more than 40% of those in the fiber direction) that cannot be attributed to nonparallel muscle fibers (MF).

Therefore, the purpose of this paper is to suggest a realistic pseudo-active kinematic law coupling the passive connective tissue to the active MF, which may explain the contribution of the collagen network to the two following mechanisms: (i) the normal systolic wall thickening, and (ii) the developed pseudo-active tension in the cross-fiber direction. The three-dimensional constitutive law including this coupling effect, and considering the myocardium as an incompressible hyperelastic material is presented. Futhermore, the proposed constitutive law for living tissue was applied to simple cases as, free contraction, uniaxial and equibiaxial extensions of a rectangular sample assuming negligible body forces and inertia effects.

2 Microstructure of the Cardiac Tissue

2.1 Muscle Fiber Organization

Anatomical observations have shown that the cardiac muscle tissue has a highly specialized architecture [12]. This structure is composed primarily of cardiac muscle cells, or myocytes that are 80 to 100 μm in length and are roughly cylindrical with cross-sectional dimensions of 10 to 20 μm. These cells are arranged in a more or less parallel weave that we idealize as "muscle fibers" (MF). We shall denote the local direction of this group of cells by the unit vector $\mathbf{f}$ and refer to it also as the local "fiber" direction with the understanding that individual continuous MF do not really exist. Experimental measurements have shown that the MF direction field defines paths on a nested family or toroidal surfaces of revolution in the wall of the heart [12]. These results show a continuously changing orientation $\mathbf{f}$ of the MF through the wall, circumferential near the midwall and progressively more inclined with respect to the equatorial plane when moving toward either the epicardium or the endocardium.

2.2 The Cardiac Connective Tissue Organization

Myocytes and coronary blood vessels are embedded in a complex extracellular matrix which consists of collagen and elastin, mainly. Caulfield and Janicki [1] used the scanning electron microscope (SEM) to reveal the basic organization of this connective tissue network. Their studies on the connective tissue of mammalian heart muscle give the description of the extracellular structures and their

arrangement relative to cardiac muscle cells. They described the three following classes of connective tissue organization: (i) interconnections between myocytes, (ii) connections between myocytes and capillaries and, (iii) a collagen weave surrounding group of myocytes. When viewed by SEM, groups of myocytes can be seen to be encompassed by a rather prominent meshwork of fibrillard collagen, and short collagen struts attach the myocytes subjacent to this meshwork to it.

3 Constitutive Law in Continuum Mechanics

3.1 Coupling between Muscle Fibers and Collagen Network

Extrapolations from the MF arrangement to the myocardial stress are realistic if we take into account the effect of the connective tissue. Based on the previous SEM observations, we proposed a connective tissue organization illustrated in Fig. 1. We assume that the MF are roughly cylindrical, and that two adjacent MF running on the tangential plane of the ventricular wall are surrounded by inextensible collagen bundles. So, during the contraction, the MF diameter increases and because the collagen bundles are inextensible, the adjacent MF become closer. Thus, the pseudo-active kinematic relationship between the extension ratios in the fiber and cross-fiber directions (noted λ_f and λ_{cf}=D'/D, respectively (see Fig.1) is given by $h(\lambda_f, \lambda_{cf}) = 0$ with:

$$h(\lambda_f, \lambda_{cf}) = 1 - \lambda_{cf} + (\pi - 2)(1 - \lambda_f^{-1/2})\frac{a}{D} \tag{1}$$

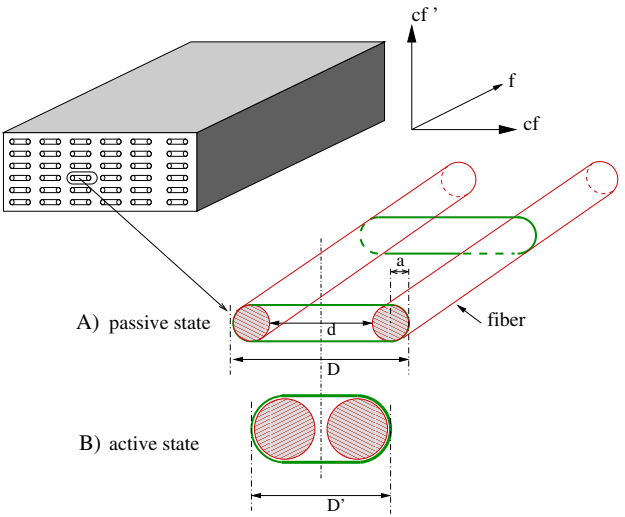

Fig. 1. Schematic illustrations of the sample of myocardium and the internal pseudo-active kinematic constraint induced by the collagen network surrounding the muscle fibers. A) Before contraction (or passive state). B) After or during contraction (or active state)

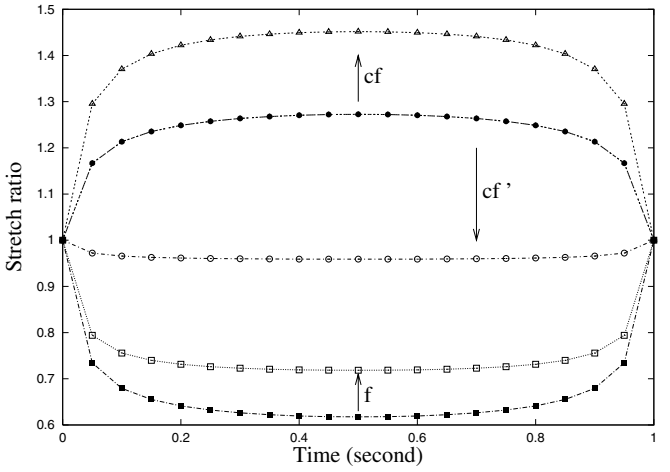

Fig. 2. Free contraction test with $\beta(t) = sin^2(\pi t)$: effect of the pseudo-active kinematic constraint. The empty and full symbols indicate that the coupling effect is acting or not, respectively. The fiber and cross-fiber directions are noted (f), (cf) and (cf ') and are defined in Fig. 1. Arrows show the curve modification when the pseudo-active kinematic constraint behaves

where $D = 4a + d$ in which a is the initial MF radius and d is the distance between the two adjacent MF.

3.2 Myocardium under Internal Pseudo-Active Kinematic Constraint

To be consistent with our mathematical formulation, the letter Φ is used for the non elastic gradient tensor and the letter $\mathbf{F}$ is used for the elastic gradient tensor. The activation of the MF changes the properties of the material and at the same time contracts the muscle itself. To have a continuous elastic description during the activation of the tissue, we used an approach similar to the one proposed by Taber [9], Lin and Yin [6]. From its passive state with zero residual stress P, the free activation of the muscle fibers is modelised by the following two transformations (Fig. 3): the first one (from state P to virtual state A_0) changes the material properties without changing the geometry, and the second one (from A_0 to A) contracts the muscle without changing the properties of the material. Thus, the former is not an elastic deformation and is described by the gradient tensor $\Phi_{PA_0} = \mathbf{I}$ where $\mathbf{I}$ is the identity matrix. In that first transformation, only the strain energy function is modified using an activation function $\beta(t)$, where t is the cardiac cycle time. The second transformation is an elastic deformation caused only by the active tension delivered by the fibers, and takes care of the internal kinematic constraint (Eq.(1)). This last transformation is described by the gradient tensor $\mathbf{F}_{A_0A}$. Thus the transformation from state P to state A is a non elastic transformation ($\Phi_{PA} = \Phi_{PA_0}\mathbf{F}_{A_0A}$), but can be

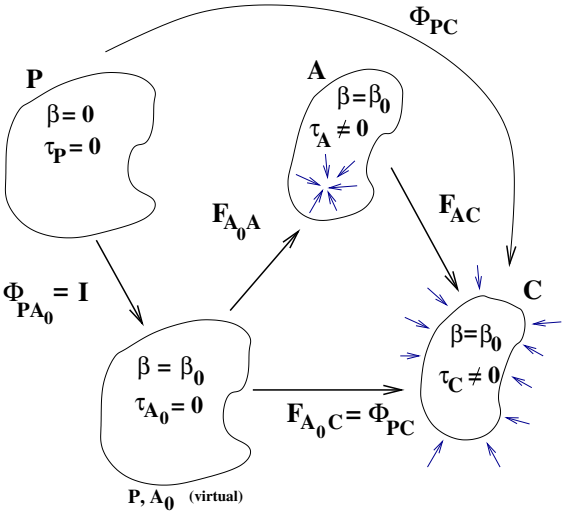

Fig. 3. Description of the active rheology in continuum mechanics (see text for more details)

treated mathematically as an elastic one because $\Phi_{PA} = \mathbf{F}_{A_0A}$. Finally, external loads are applied to state A deforming the body through into C (Fig. 3). The change of the material properties of the myocardium during the cardiac cycle is described by a time-dependent strain-energy function per unit volume of state P noted $W(\mathbf{E}_{PH}, t)$:

$$W(\mathbf{E}_{PH}) = -\tfrac{1}{2}\, p_H (I_3(\mathbf{E}_{PH}) - 1) + W^*(\mathbf{E}_{PH}) + \delta_{AH}\, W_{\substack{pseudo \\ active}}(\mathbf{E}_{PH}) \qquad (2)$$

$$\text{with} \qquad W^*(\mathbf{E}_{PH}) = W_{pas}(\mathbf{E}_{PH}) + \beta(t)\, W_{act}(\mathbf{E}_{PH}) \qquad (3)$$

where $\mathbf{E}_{PH}$ is the Green's strain tensor at an arbitrary state H calculated from the zero-stress state P (the state H could be one of the states A_0, A or C shown in Fig. 3), p_H is the Lagrangian multiplier resulting of the incompressibility condition $I_3(\mathbf{E}_{PH}) = \det \mathbf{C}_{PH} = 1$, where $\mathbf{C}_{PH}$ is the right Cauchy-Green strain tensor ($\mathbf{C}_{PH} = 2\mathbf{E}_{PH} + \mathbf{I}$), W_{pas} represents the contribution of the surrounding collagen matrix and of the passive fiber components, W_{act} arises from the change of rheology during muscular contraction, and $\beta(t)$ is an activation function equal to zero at end-diastolic state and equal to one at end-systolic state ($0 \leq \beta(t) \leq 1$). The scalar δ_{AH} is equal to one if state H is the state A and zero if the two states H and A are distinct. The pseudo-active strain energy function expressed in the last term of the right hand side of the Eq.(2) is introduced in order to satisfy the kinematic condition (Eq.(1)), and is given by:

$$W_{\substack{pseudo \\ active}}(\mathbf{E}_{PH}) = -\frac{1}{2} q_H\, h(\mathbf{E}_{PH}) \qquad (4)$$

The scalar q_H introduced in Eq.(4) is an additional indeterminate Lagrange multiplier. The function $h(\mathbf{E}_{PH})$ defined in Eq.(1), may be rewritten in terms

of the strain invariants as:

$$h(\mathbf{E}_{PH}) = 1 - I_6^{1/2} + (\pi - 2)\,(1 - I_4^{-1/4})\,\frac{a}{D} \tag{5}$$

where I_4 and I_6 are two strain invariants given by $I_4(\mathbf{E}_{PH}) = \mathbf{f}_P \cdot \mathbf{C}_{PH} \cdot \mathbf{f}_P$ and $I_6(\mathbf{E}_{PH}) = \mathbf{f}_P^{\perp} \cdot \mathbf{C}_{PH} \cdot \mathbf{f}_P^{\perp}$ in which the fiber and the perpendicular fiber directions are respectively characterized in state P by the unit vectors $\mathbf{f}_P$ and $\mathbf{f}_P^{\perp}$. In an arbitrary deformed state H, the direction of these two unit vectors are noted $\mathbf{f}_H$ and $\mathbf{f}'_H$ and are respectively defined by $\mathbf{f}_H = \Phi_{PH} \cdot \mathbf{f}_P / \parallel \Phi_{PH} \cdot \mathbf{f}_P \parallel$ and $\mathbf{f}'_H = \Phi_{PH} \cdot \mathbf{f}_P^{\perp} / \parallel \Phi_{PH} \cdot \mathbf{f}_P^{\perp} \parallel$. The superscript '$T$' is used for transpose matrix and $\parallel\ \parallel$ stands for the euclidian norm. Note that I_4 and I_6 are directly related to the fiber and cross-fiber extension ratios ($I_4 = \lambda_f^2$ and $I_6 = \lambda_{cf}^2$). In our notations, λ_f is related to the fiber direction $\mathbf{f}_H$, and λ_{cf} to the cross-fiber direction $\mathbf{f}'_H$ (Fig. 1). We treat the myocardium as a homogeneous, incompressible, and hyperelastic material transversely isotropic with respect to the local MF direction. In this study, the passive strain-energy function is [6]

$$W_{pas}(\mathbf{E}_{PH}) = C_1^p(e^Q - 1) \tag{6}$$

$$\text{with} \qquad Q = C_2^p(I_1 - 3)^2 + C_3^p(I_1 - 3)(I_4 - 1) + C_4^p(I_4 - 1)^2 \tag{7}$$

For the active strain-energy we modified the function found by Lin and Yin [6] by substracting the "beating term":

$$W_{act}(E_{PH}) = C_1^a(I_1 - 3)(I_4 - 1) + C_2^a(I_1 - 3)^2 + C_3^a(I_4 - 1)^2 + C_4^a(I_1 - 3) \tag{8}$$

where $(C_i^p, \quad i = 1, \cdots, 4)$ and $(C_i^a, \quad i = 1, \cdots 4)$ are material constants and I_1 is the first principal strain invariant given by $I_1(\mathbf{E}_{PH}) = tr\,\mathbf{C}_{PH}$. The beating term is defined as the part of the active strain-energy function responsible for the change of geometry when the muscle is activated and submited to no external loading. To incorporate the beating behavior, the time-dependant beating tension $\beta(t)\,T^{(0)}$ was applied in the deformed fiber direction.

In our approach, the active loaded state C of the myocardial tissue is obtained in two steps. In the first step, and at a given degree of activation β, we derived and quantified the internal pseudo-active stresses by looking the free contraction configuration of the tissue (state A, Fig. 3). Then, in a second step, we applied the external loads on the active myocardial tissue under the internal pseudo-active stresses previously found.

Step 1: Determination of the Free Contraction State A

During the cardiac cycle and at a given degree of activation β, the Cauchy stress tensor in state A (noted $\boldsymbol{\tau}_A$) is given by:

$$\boldsymbol{\tau}_A = -p_A\mathbf{I} + \Phi_{PA}\frac{\partial W^*(\mathbf{E}_{PA})}{\partial \mathbf{E}_{PA}}\Phi_{PA}^T + \beta(t)T^{(0)}\mathbf{f}_A \otimes \mathbf{f}_A + \boldsymbol{\tau}_A^{\substack{pseudo\\active}} \tag{9}$$

$$\text{with} \qquad \boldsymbol{\tau}_A^{\substack{pseudo\\active}} = \boldsymbol{\Phi}_{PA} \frac{\partial W_{\substack{pseudo\\active}}(\mathbf{E}_{PA})}{\partial \mathbf{E}_{PA}} \boldsymbol{\Phi}_{PA}^T \tag{10}$$

where the symbol $\otimes$ denotes the tensor product. The postulated mechanical coupling law (Eq.(5)) induces, during the contraction, a pseudo-active stress tensor:

$$\boldsymbol{\tau}_A^{\substack{pseudo\\active}} = T_A^f \, \mathbf{f}_A \otimes \mathbf{f}_A + T_A^{cf} \, \mathbf{f}'_A \otimes \mathbf{f}'_A \tag{11}$$

These two stress tensor components T_A^f and T_A^{cf} are activation-dependent and behave as some internal tensions in the fiber and cross-fiber directions of unit vectors $\mathbf{f}_A$ and $\mathbf{f}'_A$, respectively. These pseudo-active tensions are defined by:

$$T_A^f = 2 \frac{\partial W_{\substack{pseudo\\active}}}{\partial I_4} \parallel \boldsymbol{\Phi}_{PA} \cdot \mathbf{f}_P \parallel^2 \quad ; \quad T_A^{cf} = 2 \frac{\partial W_{\substack{pseudo\\active}}}{\partial I_6} \parallel \boldsymbol{\Phi}_{PA} \cdot \mathbf{f}_P^{\perp} \parallel^2 \tag{12}$$

Step 2: Determination of the Physiological Active Loaded State C
These previously found internal pseudo-active tensions T_A^f and T_A^{cf} were introduced in the expression of the stress tensor at loaded state C. Therefore, at a fixed time (or activation β) of the cardiac cycle, the Cauchy stress tensor in the physiological state C (noted $\boldsymbol{\tau}_C$) is given by:

$$\boldsymbol{\tau}_C = -p_C \mathbf{I} + \boldsymbol{\Phi}_{PC} \frac{\partial W^* (\mathbf{E}_{PC})}{\partial \mathbf{E}_{PC}} \boldsymbol{\Phi}_{PC}^T + \left(\beta T^{(0)} + T_A^f \right) \mathbf{f}_C \otimes \mathbf{f}_C + T_A^{cf} \, \mathbf{f}'_C \otimes \mathbf{f}'_C \tag{13}$$

The suggested constitutive law for the active myocardium (Eqs.(2)-(13)) allows to simulate the left ventricle behavior during the whole cardiac cycle. Thus, in this law: (i) the anisotropic behavior is incorporated in the expressions of passive, active and pseudo-active strain energy functions by the terms I_4 and I_6, (ii) the kinematic contraction is accounted for by a beating tension $\beta T^{(0)}$ in the fiber direction, (iii) the change of properties is expressed by the active strain energy term $\beta(t) W_{act}$, and (iv) the coupling effect between the collagen network and the MF is accounted for by the two internal pseudo-active tensions T_A^f and T_A^{cf} in the fiber and cross fiber directions $\mathbf{f}_C$ and $\mathbf{f}'_C$, respectively.

4 Results and Discussion

We simulated the loading of a thin sample of living myocardium ($1.0 \times 1.0 \times 0.1$ cm^3) in which the MF are uniformly oriented in one direction. The coefficients involved in the strain energy-function are those of Lin and Yin [6]: C_1^p=0.292 kPa, C_2^p=0.321, C_3^p=-0.260, C_4^p=0.201, C_1^a=-3.870 kPa, C_2^a=4.830 kPa, C_3^a=2.512 kPa and C_4^a=0.951 kPa. For the beating tension, a good agreement between the previous experimental results and our theoretical solution is obtained for $T^{(0)}$=0.6 kPa. Nevertheless, the control simulation was performed with a/D=0.2

and $T^{(0)}$=35 kPa. This higher value of $T^{(0)}$ is more adapted to the description of the left ventricular performance [7].

Influence of the Collagen Network on the Systolic Wall Thickening
The free contraction test is performed with no external displacement or force on the boundaries of the sample, but just in activating the tissue. In this simulation we used the following time-dependent activation function : $\beta(t) = sin^2(\pi t)$. Compare to the case where the kinematic constraint is not taken into account, one can see an increase of the cross-fiber extension ratio which is in the tangential plane of the ventricular wall (Fig. 3). At the end-systolic state (i.e. when $\beta = 1$), this ratio goes from the value 1.25 if we neglect the coupling effect, to 1.45 when considering the kinematic constraint induced by the collagen. So, the connective tissue could account for 16 % of normal end-systolic wall thickness. This increase is clearly dependent of the geometrical parameter ratio a/D and the maximal beating tension $T^{(0)}$.

Influence of the Collagen Network on the Pseudo-active Tension
Table 1 shows the effect of the geometrical parameter a/D and the maximal active tension $T^{(0)}$, on the fiber and cross-fiber stresses (noted σ_{11} and σ_{22}, respectively). These effects were given in the case of an equibiaxial extension loading ($\lambda_f = \lambda_{cf} = 1.2$) of an activated sample of myocardium ($\beta = 1$). These two stresses increase with $T^{(0)}$, but are not very sensitive to the geometrical ratio a/D. We can observe also, that by neglecting the interaction between the collagen network and the MF: (i) the cross-fiber stress is not affected by the amplitude of the beating tension, and (ii) the stress ratio σ_{22}/σ_{11} decreases when $T^{(0)}$ increases. These results mean that the usual strain-energy functions considered for the myocardium are not able to generate any transverse pseudo-active tension.

Moreover, the results obtained for the uniaxial tests of an active or a passive sample, with or without the effect of the collagen on the MF, are shown in Fig. 4. Because the coupling effect between the collagen and the MF is an active mechanism, the passive stress-strain relations are not affected by the kinematic constraint. The mechanical properties of the active tissue, in the fiber and cross-fiber directions, become comparable when the coupling effect acts.

5 Conclusion

This study shows that the connective tissue skeleton in the normal and pathological left ventricle may have a large influence on the cardiac performance. A new constitutive law has been developed for large deformations of an incompressible hyperelastic, and anisotropic living myocardium. This work is based on the idea that the connective tissue is physically coupled to the muscle fibers which seems reasonable with regard to the available observations. Nevertheless, additional experimental works must be done in order to support this assumption and to study thoroughly the spatial organization of the myocardial collagen fibrils under normal and pathological conditions.

Table 1. Equibiaxial test: effect of active tension $T^{(0)}$ and geometrical parameter a/D

a/D \ T_0 (kPa)		5	15	25	35	45
0.10	σ_{22}/σ_{11} (%)	50.92	53.73	57.65	60.25	61.90
	σ_{22} (kPa)	5.94	11.44	17.78	24.32	30.88
0.15	σ_{22}/σ_{11} (%)	51.44	54.56	58.60	61.30	63.01
	σ_{22} (kPa)	5.97	11.48	17.80	24.31	30.84
0.20	σ_{22}/σ_{11} (%)	51.94	55.33	59.47	62.25	64.04
	σ_{22} (kPa)	6.00	11.51	17.79	24.25	30.73
No kinematic constraint	σ_{22}/σ_{11} (%)	36.78	19.88	13.62	10.36	8.36
	σ_{22} (kPa)	4.32	4.32	4.32	4.32	4.32

Acknowledgments. This work was performed within the framework of the joint incentive action "Beating Heart" of the research group ISIS, ALP and MSPC of the French National Center for Scientific Research (CNRS). It is partly granted by the Région Rhône Alpes, through the AdéMO project and by the Lipha Santé Company, a subsidiary of the group MERCK KGaA.

References

1. J. B. Caulfield and J. S. Janicki. Structure and function of myocardial fibrillar collagen. *Technology and Health Care.*, IOS Press (5):95–113, 1997.
2. R. S. Chadwick, A. Tedgui, J.B Michel, J. Ohayon, and B. I Levy. Phasic regional myocardial inflow and outflow : comparison of theory and experiments. *Am. J. Physiol.*, 258:H1687–1698, 1990.
3. K.D. Costa, P.J. Hunter, J.S. Wayne, L.K. Waldman, J.M. Guccione, and A.D. McCulloch. A three-dimensional finite element method for large elastic deformations of ventricular myocardium: Part II - Prolate spheroidal coordinates. *ASME J. Biomech. Eng*, 118:464–470, 1996.
4. J.M. Huyghe, D.H. van Campen, T. Arts, and R.M. Heethaar. A two-phase finite element model of the diastolic left ventricle. *J. Biomech.*, 24:527–538, 1991.

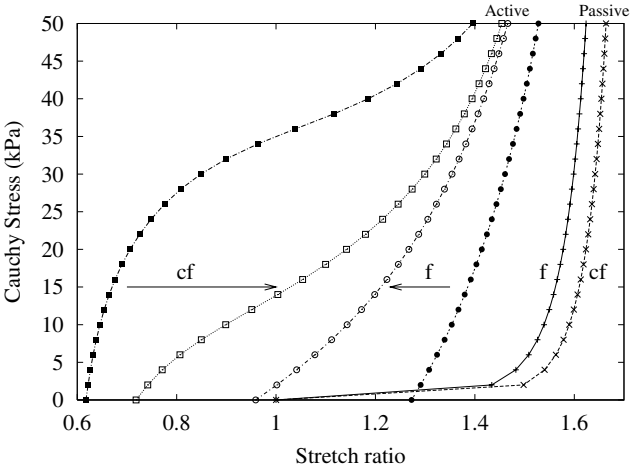

Fig. 4. Active and passive uniaxial extension tests: effect of the pseudo-active kinematic constraint. The empty and full symbols indicate that the coupling effect is acting or not, respectively. The fiber and cross-fiber directions noted (f) and (cf) are defined in Fig. 1. Arrows show the curve modification when the pseudo-active kinematic constraint behaves

5. I.J. LeGrice IJ, Y. Takayama, and J.W.J. Covell. Transverse shear along myocardial cleavage planes provides a mechanism for normal systolic wall thickening. *Circ. Res.*, 77:182–193, 1995.
6. D.H.S. Lin and F.C.P. Yin. A multiaxial constitutive law for mammalian left ventricular myocardium in steady-state barium contracture or tetanus. *J. Biomech. Eng.*, 120:504–517, 1998.
7. J. Ohayon, H. Cai, P.S. Jouk, Y. Usson, and A. Azancot. A model of the structural and functional development of the normal human fetal left ventricle based on a global growth law. *Comp. Meth. Biomech. Biomed. Eng.*, 2002.
8. J. Ohayon and R.S. Chadwick. Effects of collagen microstructure on the mechanics of the left ventricle. *Biophys. J.*, 54:1077–1088, 1988.
9. L.A. Taber. On a nonlinear theory for muscle shells: Part II- Application to the beating left ventricle. *J. Biomech. Eng.*, 113:63–71, 1991.
10. M.A. Rossi. Connective tissue skeleton in the normal left ventricle and in hypertensive left ventricular hypertrophy and chronic chagasis myocarditis. *Med. Sci. Monit.* 7(4):820–832, 2001.
11. S.J. Sarnoff, E. Braunwald, G.H. Jr. Welch, R. B. Case, W. N. Stainsby, and R. Macruz. Hemodynamic determinants of oxygen consumption of the heart with special reference to the tension-time index. *Am. J. Phsysiol.*, 192:148–156, 1958.
12. D.D. Streeter. Gross morphology and fiber geometry of the heart. In R. M. Berne et al., editor, *Handbook of physiology*, volume 1, pages 61–112, Bethesda MD, 1979. American Physiological Society.
13. T.P. Usyk, J.H. Omens, A.D. McCulloch Regional septal dysfunction in a three-dimensional computational model of focal myofiber disarray. *Am. J. Physiol. Heart Circ. Physiol.*, 281: H506–H514, 2001